CONSTRUCTION OF 3D LUNG IMAGE MORPHOLOGY USING 3D DISTANCE REGULARIZED LEVEL SET

Chuen Rue Ng[1], Joel Chia Ming Than[1], Omar Mohd Rijal[2], Rosminah Md Kassim[3], Ashari Yunus[4] and Norliza Mohd Noor[1]
[1]Razak Faculty of Technology and Informatics, UniversitiTeknologi Malaysia, Kuala Lumpur, Malaysia
[2]Faculty of Science, Universiti of Malaya, Petaling Jaya, Malaysia
[3]Department of Diagnostics Imaging, Kuala Lumpur Hospital, Kuala Lumpur, Malaysia
[4]Institute of Respiratory Medicine, Kuala Lumpur Hospital, Kuala Lumpur, Malaysia
E-Mail: norliza@utm.my

ABSTRACT

The World Health Organization (WHO) has stated in its report that lung disease is a wide spread in Malaysia which caused 2.77% of total death in Malaysia making it the 6th main cause of death in Malaysia. One of the lung diseases included in the list is interstitial lung disease (ILD). ILD includes an extensive group of disorders which leads breathing complications as a result of the alteration and fibrosis to anatomical structures in the alveolar structures. Therefore, diagnosis and analysis of ILD can be performed by segmenting the lung morphology on CT scans images. This study aims to construct a 3D lung image morphology using 3D distance regularized level set evolution (DRLSE). The 3D performance evaluations for normal lungs on average yielded better results than that of ILD lungs with a Dice's similarity coefficient of 93.19%. The constructed lungs from 3D DRSLE has good representation of the segmented normal lungs while suggesting deformities in segmented ILD lungs.

Keywords: level set, 3D segmentation, CT scan.

INTRODUCTION

The World Health Organization (WHO) has stated in its report that lung disease is a wide spread in Malaysia which caused 2.77% of total death in Malaysia making it the 6th main cause of death in Malaysia [1]. One of the lung diseases included in the list is interstitial lung disease (ILD). ILD includes an extensive group of disorders which leads breathing complications as a result of the alteration and fibrosis to anatomical structures in the alveolar structures [2-3]. Therefore, diagnosis and analysis of ILD can be performed by segmenting the lung morphology on CT scans images [4]. Generally, image segmentation can be separated into two different categories according to how the shape is represented which is either explicitly or implicitly [5]. Explicit image segmentation represents a shape by its boundary such as snake algorithm [6] whereas implicit image segmentation represents a shape by its content for example level set segmentation. An advantage of implicit representation over explicit representation is that the splitting of a shape into several shapes is easier and more straight forward making it suitable for the segmentation of lungs [7]. Introduced by Dervieux and Thomasset [8-9] and then by Osher and Sethian [10], level set represents a contour as a level set function (LSF) and the contour motion can be controlled by evolving the LSF. The level set evolution in a conventional method however will cause irregularities which can be solved by reinitialization between evolution processes [11-14]. A variation of level set which is the distance regularized level set evolution (DRLSE) has been introduced by Li *et al.* which requires no reinitialization [15] and has wide applications including medical image segmentation [16-18]. This study aims to construct a 3D lung image morphology using modified 3D distance regularized level set.

MATERIALS AND METHODS

Data acquisition

A total of 3 healthy individuals and 3 ILD patients' high-resolution computed tomography (HRCT) Thorax images were obtained from Kuala Lumpur Hospital. Each volume consists of approximately 30 HRCT image slices and they were collected from Siemens SomatomPlus4 CT scanner. The image slices have a slice thickness of 10 mm and are saved in 512×512 DICOM format.

3D segmentation

The DICOM images were first being pre-processed using image morphology. This is mainly to remove non-body pixels in an image. A simple Otsu thresholding was also carried out to remove pixels inside the body that has a large Hounsfield Unit (HU) difference than that of the lungs (which has a low HU). The results of the pre-processing were the lung and some other components inside the body that has low HU such as trachea.

Next, all the 2D HRCT images slices of one patient were stacked together to form into a 3D volume. Besides, 10 empty slices were added before and after the 3D volume as a buffer for the initialization of 3D DRLSE. Since some of the HRCT images are taken starting from the lungs, the buffer caused the initialization outside of the lungs. This is especially important because of the front-propagation nature of the DRLSE. If the zeroth level set is initialized within the lungs, DRLSE would not work and only the edge of the lungs which have huge HU difference with the surrounding are segmented.

After that, the buffered and stacked lungs are being initialized with a cuboid shape as shown in Figure-2.

The level set evolution will proceed until either there is no volume change in 3 iterations or until the pre-determined number of iterations. The volume of the lungs is calculated by the total pixels available in the whole lungs segmented by DRLSE.

The final step of the algorithm is to perform 3D "box" smoothing before the lungs are being rendered. The smoothing of the lungs is mostly for aesthetic purposes as it will reduce the overall lung volume by a small margin. The flow chart for the construction of 3D lungs images with DRLSE can be seen in Figure-1.

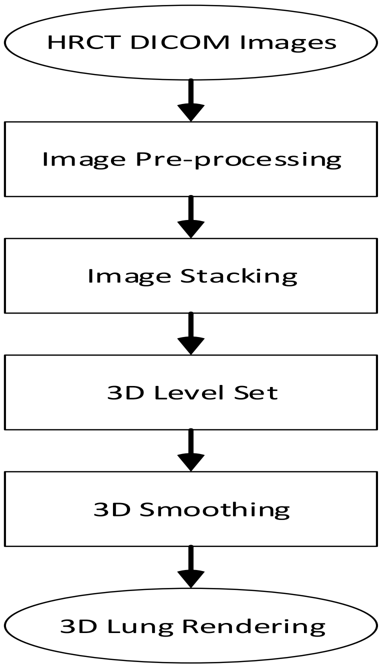

Figure-1. Flow chart for the construction of 3D lung images with DRLSE.

Performance evaluation

The performance of the 3D image segmentation (before smoothing) is evaluated by using relative volume difference (RVD), Jaccard's Index (JI) and Dice Similarity Coefficient (DSC). All three performance evaluations are performed in 3D. For all evaluations, we assume A as the automated 3D segmentation and B as the ground truth (GT) or manual delineation by a radiologist. The manual delineation was traced in 2D and stacked together to form a 3D ground truth stacked lungs volume. The ground truth stacked lungs volume is also buffered with 10 empty slices before and after the volume to enable the calculation of JI and DSC in 3D. RVD is the computation of the volume difference of the automated segmentation relatively to the ground truth [19] and is given in the following equation;

$$\text{RVD} = \frac{A-B}{B} \times 100\%. \quad (1)$$

JI determines the ratio of intersect region to the union region between A and B [20] and is given as follow;

$$\text{JI} = \frac{A \cap B}{A \cup B} \times 100\%. \quad (2)$$

DSC shows the degree of intersect region to the average region of A and B [21] as shown in equation (3);

$$\text{DSC} = \frac{A \cap B}{A + B} \times 200\%. \quad (3)$$

RESULTS AND DISCUSSIONS

Figure-2 shows the evolution of 3D distance regularized level set. The cuboid initialization deforms slowly to become the shape of lungs. The smoothing process that followed up can be seen in Figure-3. It is worth noticing that the size or volume of the lungs decreased slightly.

The 3D DRLSE results and their respective ground truth stacked lungs for the 6 patients can be seen in both Figure-4 (normal patients) and Figure 5 (ILD patients).

While the 3D smoothing helps the presentation of the normal lungs, it happened to be quite the opposite for the ILD lungs. As seen in Figure-6, the tiny crevices on the edge of the lungs indicated by arrows on the intermediate smoothing images are amplified into bigger cuts from the lungs. Although these spots might not be the exact spots that have been infected by ILD, the smoothing effects in turns helps in differentiating between normal lungs and ILD lungs due to the fact that all three ILD lungs has obvious deformity of some sort at the final 3D rendering of the lungs.

As seen in Table-1, the 3D performance evaluations for normal lungs on average yielded better results than that of ILD lungs. This is because normal lungs have less scattered pixels caused by deformities as suggested from previous study [22]. All in all, 3D DRLSE segmented lungs on both normal and ILD lungs has low RVE, high JI and high DSC.

ISSN 1819-6608
ARPN Journal of Engineering and Applied Sciences

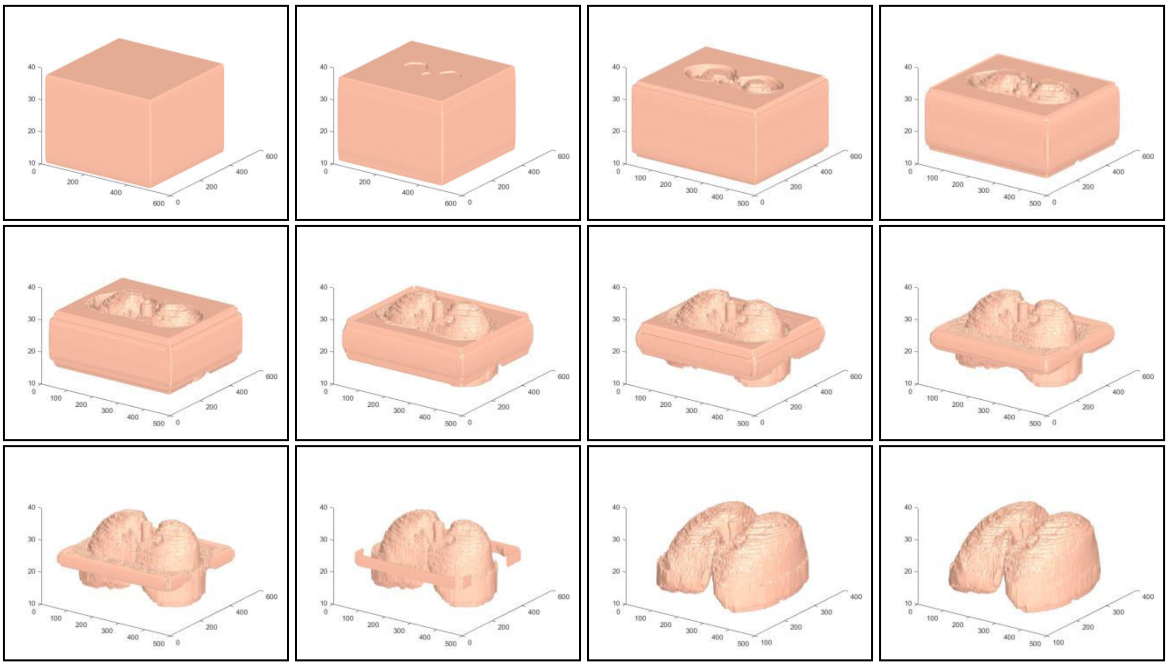

Figure-2. Example of 3D DRLSE on normal lungs.

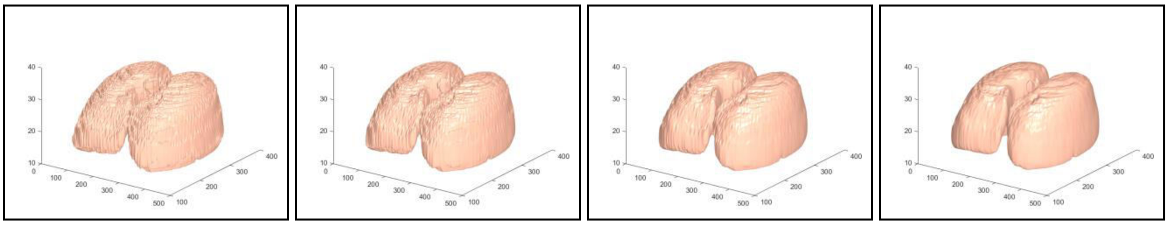

Figure-3. Example of 3D smoothing process onnormal lungs

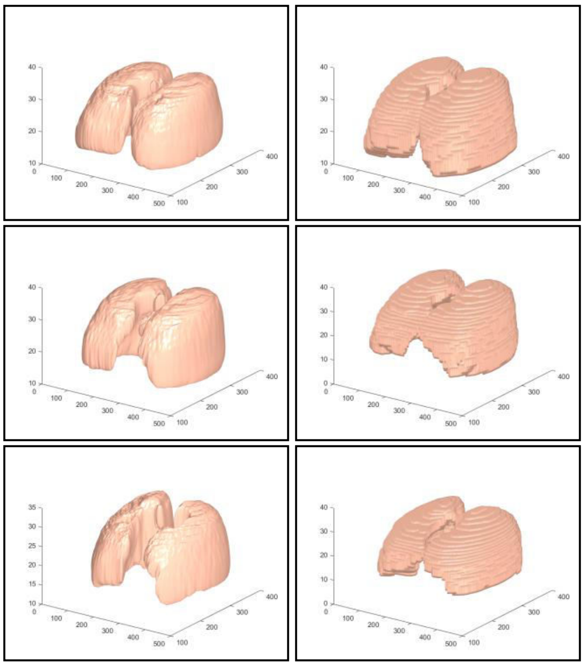

Figure-4. 3D DRLSE results and stacked GT for normal lungs.

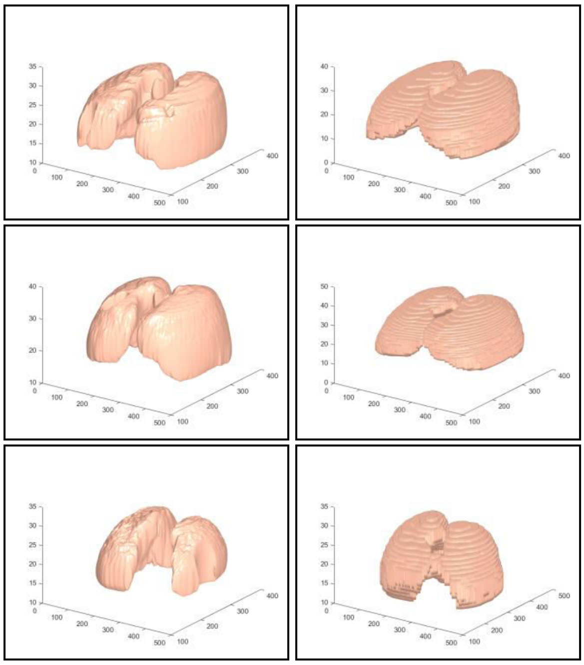

Figure-5. 3D DRLSE results and stacked GT for ILD lungs.

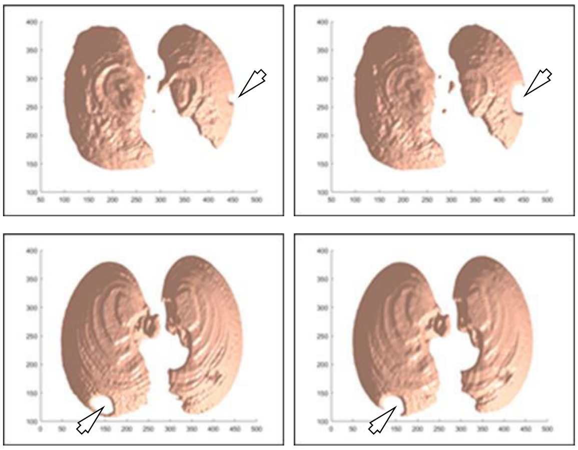

Figure-6. Smoothing effects on ILD lungs. Left: intermediate smoothing results. Right: finalsmoothing results.

Table-1. Results for 3D DRLSE on both normal and ILD lungs.

Normal	**RVE** (%)	**JI** (%)	**DSC** (%)
1	0.75	91.81	95.73
2	0.21	89.19	94.28
3	3.97	81.11	89.57
Average	**1.64**	**87.37**	**93.19**
ILD	**RVE** (%)	**JI** (%)	**DSC** (%)
1	3.83	75.49	86.03
2	2.20	88.47	93.88
3	8.09	83.81	91.19
Average	**4.71**	**82.59**	**90.37**

CONCLUSIONS

The automated 3D DRLSE proposed are capable of segmenting and constructing 3D lungs that has high similarity and low error when comparing to the ground truth. The smoothing effects improves the appearance of the segmented normal lungs while suggesting deformities in segmented ILD lungs. Future studies include increasing dataset preferably from global database and ILD detection based on 3D lungs segmented using 3D DRLSE.

ACKNOWLEDGEMENT

Research is supported by the Universiti Teknologi Malaysia Research University, and Ministry of Higher Education Malaysia.

REFERENCES

[1] W. H. Organization and others. 2014. Global status report on noncommunicable diseases 2014. World Health Organization.

[2] M. I. Schwarz, R. A. Matthay, S. A. Sahn, R. E. Stanford, B. L. Marmorstein and D. J. Scheinhorn. 1976. Interstitial lung disease in polymyositis and dermatomyositis: analysis of six cases and review of the literature. Medicine (Baltimore). 55(1): 89-104.

[3] T. Peros-Golubicic and O. P. Sharma. 2006. Clinical atlas of interstitial lung disease. Springer Science & Business Media.

[4] E. Henne, J. C. Anderson, N. Lowe and S. Kesten. 2012. Comparison of human lung tissue mass measurements from ex vivo lungs and high-resolution CT software analysis," BMC Pulm. Med. 12(1): 18.

[5] D. Cremers. 2015. Image segmentation with shape priors: Explicit versus implicit representations. Handb. Math. Methods Imaging. pp. 1909-1944.

[6] M. Kass, A. Witkin and D. Terzopoulos. 1988. Snakes: Active contour models. Int. J. Comput. Vis. 1(4): 321-331.

[7] D. Cremers, M. Rousson and R. Deriche. 2007. A review of statistical approaches to level set

segmentation: integrating color, texture, motion and shape.Int. J. Comput. Vis. 72(2): 195-215.

[8] A. Dervieux and F. Thomasset. 1981. Multifluid incompressible flows by a finite element method. In: Seventh International Conference on Numerical Methods in Fluid Dynamics. pp. 158-163.

[9] Dervieux and F. Thomasset. 1980. A finite element method for the simulation of Rayleigh-Taylor instability. in Approximation methods for Navier-Stokes problems, Springer. pp. 145-158.

[10] S. Osher and J. A. Sethian. 1988. Fronts propagating with curvature-dependent speed: algorithms based on Hamilton-Jacobi formulations.J. Comput. Phys. 79(1): 12-49.

[11] J. A. Sethian and others. 2003. Level set methods and fast marching methods.J. Comput. Inf. Technol. 11(1): 1-2.

[12] S. Osher and R. Fedkiw. 2006. Level set methods and dynamic implicit surfaces. vol. 153. Springer Science & Business Media.

[13] M. Sussman and E. Fatemi. 1999. An efficient, interface-preserving level set redistancing algorithm and its application to interfacial incompressible fluid flow.SIAM J. Sci. Comput. 20(4): 1165-1191.

[14] M. Sussman, P. Smereka, and S. Osher. 1994. A level set approach for computing solutions to incompressible two-phase flow.J. Comput. Phys. 114(1): 146-159.

[15] Li C., Xu C. Gui and M. D. Fox. 2010. Distance regularized level set evolution and its application to image segmentation. IEEE Trans. image Process. 19(12): 3243-3254.

[16] Li R., Huang Z., Ding J. C.,Gatenby D. N., Metaxas and J. C. Gore. 2011. A level set method for image segmentation in the presence of intensity in homogeneities with application to MRI.IEEE Trans. Image Process. 20(7): 2007-2016.

[17] R. Ng, N. M. Noor and O. M. Rijal. 2016. Level set segmentation for brain region using CT scan images. In: Biomedical Engineering and Sciences (IECBES), 2016 IEEE EMBS Conference on. pp. 166-169.

[18] K. N. B. Prakash, S. Zhou, T. C. Morgan, D. F. Hanley and W. L. Nowinski. 2012. Segmentation and quantification of intra-ventricular/cerebral hemorrhage in CT scans by modified distance regularized level set evolution technique. Int. J. Comput. Assist. Radiol. Surg. 7(5): 785-798.

[19] J. O. Bennett and W. L. Briggs. 2008. Using and understanding mathematics: A quantitative reasoning approach. Pearson Addison Wesley Reading, MA.

[20] P. Jaccard. 1908. Nouvelles recherches sur la distribution florale.

[21] Gallagher. COMPAH documentation. User's Guid. Appl. Publ. published at.

[22] C. R. Ng, J. C. M. Than, N. M. Noor, O. M. Rijal, R. M. Kassim and A. Yunus. 2017. Preliminary 3D performance evaluation on automatic lung segmentation for interstitial lung disease using high resolution computed tomography. In: Region 10 Conference, TENCON 2017-2017 IEEE. pp. 187-191.